International Journal of Mechatronics, Electrical and Computer Technology

Vol. 4(13), Oct, 2014, pp. 1452-1472, **ISSN**: 2305-0543
Available online at: http://www.aeuso.org

A Comparative Study between RISE Feedback and Twisting Second Order Sliding Mode Controllers for a 3 DOF Robot Manipulator

Marzieh Yazdanzad* and Alireza Khosravi

Department of Electrical and Computer Engineering, Noshirvani University of Technology, Babol, Iran

*Corresponding Author's E-mail: s.yazdanzad@stu.nit.ac.ir

Abstract

The robotic control is a very popular research topic due to its wide range of applications. In this paper, the problem of position tracking control of a three degree-of-freedom (DOF) robot manipulator is investigated in presence of uncertainties and bounded external disturbances. Due to complexity of robot manipulators and system uncertainties, a robust control technique is required to solve this problem. In this paper, two different robust control schemes including twisting second-order sliding mode and robust integral of the sign of the error (RISE) feedback are designed and their performances are compared in simulation. RISE feedback is a recently developed continuous control strategy that can compensate uncertainties and bounded external disturbances and results in asymptotic trajectory tracking. To avoid selecting the gains of controllers by time-consuming trial and error method, particle swarm optimization (PSO) algorithm is used. The objective of the PSO algorithm is to detect a set of parameters that minimizes the mean of root squared error as the fitness function. A comparative assessment of both control strategies to the system performance is analyzed and discussed.

Keywords: Robust integral of the sign of the error (RISE) feedback, Twisting sliding mode, 3 DOF robot manipulator, Particle swarm optimization (PSO), Asymptotic tracking

1. Introduction

Along the last decades, robot manipulators have achieved a big breakthrough in various applications such as medicine, aerospace, automotive and other industries. They are of highly

Vol. 4(13), Oct, 2014, pp. 1452-1472, **ISSN**: 2305-0543
Available online at: http://www.aeuso.org

nonlinear dynamic systems that are inevitably subject to various uncertainties. In recent years, there has been a tremendous progress in the development of controllers for robot manipulators to achieve a precise tracking control such as computed torque control [1], adaptive control techniques [2, 3], sliding mode control (SMC), [4, 5, 6] neural network (NN) techniques [7,8] and fuzzy control [9]. Unfortunately, computed torque control method requires an accurate dynamic model of system. In fact, the performance of this technique may be significantly degraded in presence of uncertainties in the dynamic model. Adaptive controller can cope with parametric uncertainties and bounded disturbances. However, this type of controller is often confined to systems that are linear in the unknown parameters. Moreover, it requires an exact knowledge of system structure to determine the regression matrix. On the other hand, a new regression matrix should be computed for any specified plant which involves tedious computations.

Robot manipulators are complex nonlinear systems. In fact, it is almost impossible or very difficult to obtain an exact dynamic model of the robot due to the presence of uncertain elements such as nonlinear friction, parameters variations, unknown disturbances and etc. Hence, a robust strategy of control is required to deal with the mentioned uncertainties. Sliding mode control is an efficient robust control strategy that is widely applied in controlling uncertain nonlinear systems [10, 11, 12]. This technique was first proposed in the early 1950 by Emelyanov [13]. High accuracy and strong robustness against system uncertainties, as well as simplicity of design and implementation are the main advantages of this method. The basic idea of sliding mode control is first to select a proper sliding surface and then to design a control law that forces the system's state to reach and remain on the prescribed sliding surface. The most important part of sliding mode control design is the selection of the sliding surface. In the case of traditional SMC design, the sliding surface is chosen such that it has relative degree one with respect to the control input. It means that the control law acts on the first derivative of the sliding surface. Indeed, the objective of the first order sliding mode is to force the system state trajectory to move on the switching

Vol. 4(13), Oct, 2014, pp. 1452-1472, **ISSN**: 2305-0543
Available online at: http://www.aeuso.org

surface $s(t) = 0$. Over the last two decades, the higher-order sliding mode (HOSM) technique has been developed for the robust control of uncertain nonlinear systems with relative degree two and higher [14-19]. The basic idea of HOSM control is to act on higher order time derivatives of the sliding surface. This approach preserves the main advantages of conventional SMC and also yields better convergence accuracy and desired performance. The second-order sliding mode control is determined by $s(t) = \dot{s}(t) = 0$. In fact, in the case of second-order sliding mode, the aim is to force the system state to move on the sliding surface $s(t) = 0$, as well as to keep the first derivative of sliding surface $\dot{s}(t)$ null. It should be noted that different second-order SMC algorithms have been presented in the literature including the twisting algorithm, the super-twisting algorithm [20, 21], the sub-optimal algorithm [22], and the drift algorithm [23].

Recently, a new feedback control strategy called robust integral of the sign of the error (RISE) is proposed in [24]. This control scheme has been extensively studied because it can compensate for additive disturbances and uncertainties under the assumption that the disturbances are C^2 with bounded time derivatives by generating a continuous control signal [25, 26]. In fact, the existence of a unique integral sign term in the RISE term causes a continuous control structure which prevents the occurrence of undesirable chattering phenomenon. In [27], Patre et al. utilized this method to develop a tracking controller for a class of uncertain nonlinear systems. The RISE method is a high gain feedback tool. Motivated by this issue, in [28, 29], a NN-based feed-forward term is combined with the RISE feedback structure in order to reduce the gain values of the RISE feedback and to yield asymptotic tracking results. Also Shicheng Wang et al. in [30], designed a RISE based NN controller for a spacecraft formation within the leader follower architecture. It should be noted that the RISE feedback control scheme is inspired from second-order sliding mode. But, the RISE method is applicable to nonlinear systems with arbitrary relative degree in comparison with the second-order sliding mode which is restricted to plants with relative degree two.

Vol. 4(13), Oct, 2014, pp. 1452-1472, **ISSN**: 2305-0543
Available online at: http://www.aeuso.org

This paper presents investigation of performance comparison between twisting second-order sliding mode and RISE feedback control schemes for a three link robot manipulator tracking problem. Particle swarm optimization (PSO) is a population-based search method that can be used to find the optimal solution in a multidimensional search space. In this paper, PSO algorithm is applied to tune gains of the controllers by minimizing the root mean squared error of the robot.

The remainder of this paper is organized as follows. Section 2 presents nonlinear dynamic model of a three link robot manipulator. In section 3, the strategy of twisting second-order sliding mode as well as RISE feedback control are described. In section 4, PSO optimization technique is explained. Both of the RISE feedback and twisting sliding mode control schemes are implemented on the three link robot manipulator and the simulation results are provided in section 5. Finally, conclusions are presented in section 6.

2. Dynamic Model of Three Link Robot

The dynamics of a general rigid link manipulator having *n*-degrees of freedom in free space can be written as [31]:

$$M(q)\ddot{q} + C(q,\dot{q})\dot{q} + G(q) + \tau_d = \tau \tag{1}$$

This dynamic equation is obtained using the Euler-Lagrangian formulation. In (1) for the rigid 3-DOF robot manipulator $q(t), \dot{q}(t)$ and $\ddot{q}(t) \in R^3$ are the joint positions, velocities and accelerations vectors, respectively. $\tau \in R^3$ represents the vector of the input torque applied to the joints. $M(q) \in R^{3\times3}$ is the positive definite inertia matrix whilst $C(q,\dot{q}) \in R^{3\times3}$ is the Coriolis/centripetal matrix, and $G(q) \in R^3$ denotes the gravity vector. $\tau_d \in R^3$ denotes the vector of external disturbances and un-modeled dynamics. The configuration of the 3-link robot manipulator is shown in figure 1.

International Journal of Mechatronics, Electrical and Computer Technology

Vol. 4(13), Oct, 2014, pp. 1452-1472, **ISSN**: 2305-0543
Available online at: http://www.aeuso.org

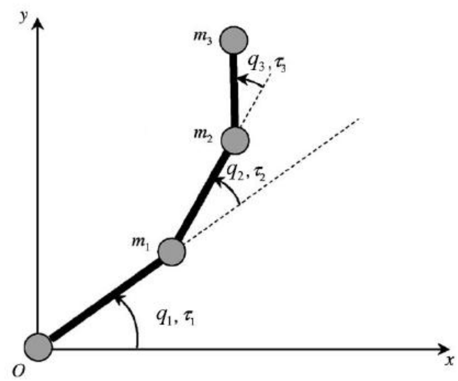

Figure 1: Three link planar robot

In this system the inertia matrix $M(q)$, the Coriolis/centripetal matrix $C(q, \dot{q})$ and the gravity vector $G(q)$ are as follows [32]:

$$M(q, \dot{q}) = \begin{bmatrix} M_{11} & M_{12} & M_{13} \\ M_{21} & M_{22} & M_{23} \\ M_{31} & M_{32} & M_{33} \end{bmatrix}$$

where

$$M_{11} = 2(d_1 + d_2 + d_3) + 2d_4 c_2 + 2d_5 c_{23} + 2d_6 c_3$$

$$M_{12} = 2(d_2 + d_3) + d_4 c_2 + d_5 c_{23} + 2d_6 c_3$$

$$M_{13} = 2d_3 + d_5 c_{23} + d_6 c_3$$

$$M_{21} = M_{12}$$

$$M_{22} = 2(d_2 + d_3) + 2d_6 c_3$$

$$M_{23} = 2d_3 + d_6 c_3$$

$$M_{31} = M_{13} \;,\; M_{32} = M_{23} \;,\; M_{33} = 2d_3$$

and

Vol. 4(13), Oct, 2014, pp. 1452-1472, **ISSN**: 2305-0543
Available online at: http://www.aeuso.org

$$C(q,\dot{q})\dot{q} = \begin{bmatrix} C_{11} & C_{12} & C_{13} \\ C_{21} & C_{22} & C_{23} \\ C_{31} & C_{32} & C_{33} \end{bmatrix} \begin{bmatrix} \dot{q}_1 \\ \dot{q}_2 \\ \dot{q}_3 \end{bmatrix}$$

where $C_{ij}, (i = 1,2,3,\ j = 1,2,3)$ are defined as follows:

$$C_{11} = -\dot{q}_2 d_4 s_2 - d_5 s_{23}(\dot{q}_2 + \dot{q}_3) - d_6 s_3 \dot{q}_3$$
$$C_{12} = -d_4 s_2(\dot{q}_1 + \dot{q}_2) - d_5 s_{23}(\dot{q}_1 + \dot{q}_2 + \dot{q}_3) - d_6 s_3 \dot{q}_3$$
$$C_{13} = -(d_5 s_{23} + d_6 s_3)(\dot{q}_1 + \dot{q}_2 + \dot{q}_3)$$
$$C_{21} = (d_4 s_2 + d_5 s_{23})\dot{q}_1 - d_6 s_3 \dot{q}_3$$
$$C_{22} = -d_6 s_3 \dot{q}_3$$
$$C_{23} = -d_6 s_3(\dot{q}_1 + \dot{q}_2 + \dot{q}_3)$$
$$C_{31} = d_5 s_{23}\dot{q}_1 + d_6 s_3(\dot{q}_1 + \dot{q}_2)$$
$$C_{32} = d_6 s_3(\dot{q}_1 + \dot{q}_2)\ ,\ C_{33} = 0$$

and

$$G(q) = \begin{bmatrix} g_1 \\ g_2 \\ g_3 \end{bmatrix}$$

$$g_1 = \frac{1}{2}a_1 c_1 m_1 g + \left(a_1 c_1 + \frac{1}{2}a_2 c_{12}\right) m_2 g + (a_1 c_1 + a_2 c_{12} + \frac{1}{2}a_3 c_{123}) m_3 g$$

$$g_2 = \left(\frac{1}{2}a_2 c_{12}\right) m_2 g + (a_2 c_{12} + \frac{1}{2}a_3 c_{123}) m_3 g$$

$$g_3 = (\frac{1}{2}a_3 c_{123}) m_3 g \qquad (2)$$

where $q = [q_1\ q_2\ q_3]^T$ and $\dot{q} = [\dot{q}_1\ \dot{q}_2\ \dot{q}_3]^T$ contain the joints displacement and velocities, respectively. m_i $(i = 1,2,3)$ are links masses and a_i $(i = 1,2,3)$ represent the lengths of the links. Meanwhile s_i, c_i, s_{ij}, c_{ij} and c_{ijk} $(i = 1,2,3,\ j = 1,2,3,\ k = 1,2,3)$ denote $\sin(q_i), \cos(q_i), \sin(q_i + q_j), \cos(q_i + q_j), \cos(q_i + q_j + q_k)$, respectively, whilst parameters d_i $(i = 1, \ldots, 6)$ are defined as follows [32]:

International Journal of Mechatronics, Electrical and Computer Technology

Vol. 4(13), Oct, 2014, pp. 1452-1472, **ISSN**: 2305-0543
Available online at: http://www.aeuso.org

$$d_1 = \frac{1}{2}[\left(\frac{1}{4}m_1 + m_2 + m_3\right)a_1^2 + I_{o1}]$$

$$d_2 = \frac{1}{2}[\left(\frac{1}{4}m_2 + m_3\right)a_2^2 + I_{o2}]$$

$$d_3 = \frac{1}{2}[\left(\frac{1}{4}m_3\right)a_3^2 + I_{o3}]$$

$$d_4 = (\frac{1}{2}m_2 + m_3)a_1 a_2$$

$$d_5 = \frac{1}{2}m_3 a_1 a_3$$

$$d_6 = \frac{1}{2}m_3 a_2 a_3 \quad (3)$$

where I_{oi} $(i = 1,2,3)$ denotes the moment of inertia of i^{th} link.

It is assumed that $q(t)$ and $\dot{q}(t)$ are measurable and $M(q), C(q,\dot{q}), G(q)$ and $\tau_d(t)$ are unknown. Furthermore, the robot manipulator dynamics given in (1) have the following properties:

Property 1: The inertia matrix $M(q)$ is symmetric, positive definite and holds true the following inequality:

$$m_1\|y\|^2 \le y^T M(q) y \le \bar{m}(q)\|y\|^2 \ \ \forall y \in R^3 \quad (4)$$

where $m_1 \in R$ is a known positive constant, $\bar{m}(q) \in R$ is a known positive function and $\|.\|$ denotes the standard Euclidean norm.

Property 2: If $q(t), \dot{q}(t) \in \mathcal{L}_\infty$, then $C(q,\dot{q}), G(q)$ are bounded. Further, if $q(t), \dot{q}(t) \in \mathcal{L}_\infty$, then the first and second partial derivatives of the elements of $M(q), C(q,\dot{q}), G(q)$ with respect to $q(t)$ exist and are bounded, and the first and second partial derivatives of the elements of $C(q,\dot{q})$ with respect to $\dot{q}(t)$ exist and are bounded as well.

Property 3: The nonlinear disturbance term and its first two time derivatives are bounded i.e., $\tau_d(t), \dot{\tau}_d(t), \ddot{\tau}_d(t) \in \mathcal{L}_\infty$.

Vol. 4(13), Oct, 2014, pp. 1452-1472, **ISSN**: 2305-0543
Available online at: http://www.aeuso.org

3. Controller Design

3.1. RISE feedback controller

Recently a novel feedback control scheme called robust integral of the sign of the error (RISE) is proposed in [24]. This method compensates for bounded disturbances or uncertainties of dynamic system using a continuous control signal. Using this technique, an asymptotic tracking is achieved without chattering problem that usually occurs in sliding mode controllers.

The objective is to design a controller for the robot manipulator that guarantees tracking of a desired trajectory which is denoted by $q_d(t) \in R^n$, in spite of uncertainties and bounded disturbances. To formulate this objective, a position tracking error, denoted by $e_1(t) \in R^n$, is defined as:

$$e_1 = q_d - q \tag{5}$$

It is assumed that the desired trajectory is designated such that $q_d{}^{(i)}(t) \in \mathcal{L}_\infty, i = 1,2, \ldots, 5$. Moreover, the filtered tracking errors are denoted by $e_2(t), r(t) \in R^n$, which are defined as follows:

$$e_2 = \dot{e}_1 + \alpha_1 e_1 \tag{6}$$

$$r = \dot{e}_2 + \alpha_2 e_2 \tag{7}$$

where $\alpha_1 \in R^{n\times n}$ is a positive constant matrix and $\alpha_2 \in R$ is a positive constant.

The continuous RISE feedback control law to attain the mentioned control objective is as follows [24]:

$$\tau(t) = (k_s + 1)e_2(t) - (k_s + 1)e_2(0) + \int_0^t [(k_s + 1)\alpha_2 e_2(\sigma) + \beta_1 sgn(e_2(\sigma))]d\sigma \tag{8}$$

where k_s and $\beta_1 \in R$ are positive constant control gains and *sgn*(.) denotes the standard sign function.

Vol. 4(13), Oct, 2014, pp. 1452-1472, **ISSN**: 2305-0543
Available online at: http://www.aeuso.org

3.2 Twisting algorithm

In last years, second-order sliding mode algorithms become very important for Variable Structure Systems (VSS) Theory. One of the most popular algorithms among the second-order sliding mode algorithms is the twisting algorithm. The twisting algorithm for the control of systems with relative degree two can be described as follows. Consider the system in the following state space form:

$$\begin{cases} \dot{x} = Ax + Bu \\ \quad y = Cx \end{cases} \tag{9}$$

where A, B and C are matrices of respective dimensions, $x \in R^n$ is the state vector and $y \in R^l$ denotes the output of the plant. The control input u of the twisting algorithm is defined as follows [33]:

$$u = c_1 sgn(e) + c_2 sgn(\dot{e}), \qquad e = r - y \tag{10}$$

where r is the command signal. Meanwhile, c_1 and c_2 are positive constant control gains, $c_1 > c_2 > 0$. A block diagram of the twisting algorithm is depicted in figure 2.

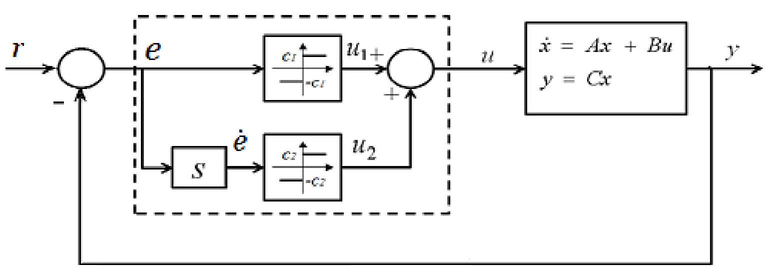

Figure 2: Block diagram of twisting algorithm

4 The Particle Swarm Optimization

4.1. PSO algorithm

PSO is a population-based optimization method inspired by the flocking and schooling patterns of birds and fish. This method consists of a swarm of particles, where each particle

Vol. 4(13), Oct, 2014, pp. 1452-1472, **ISSN**: 2305-0543
Available online at: http://www.aeuso.org

represents a potential solution. In a PSO system, each particle flies through the multidimensional search space to adjust its position according to its own previous flying experience as well as the flying experience of its neighboring particle. In other word, each particle is considered as a point in search space, in which we try to find an optimal location.

Each particle i has a position vector $X_i = (x_{i1}, x_{i2}, \dots, x_{iD})$, and a velocity vector $V_i = (v_{i1}, v_{i2}, \dots, v_{iD})$, where D represents dimension of search space. Similar to the other optimization techniques, PSO requires a fitness function to evaluate performance of each particle. Further, each particle contains a memory to store the best position in the search space ever seen by it. Velocity and position are initialized with random vectors of corresponding dimension. Trajectory of each particle in the search space is adjusted by updating the velocity, according to the best position attained so far for it, denoted by $pBest$, and also the best position obtained by any particle in the swarm, denoted by $gBest$, so far. The velocity and position of the i^{th} particle on dimension d are updated according to the following equations:

$$V_{id} = wv_{id} + k_1 r_{1d}(pBest_{id} - x_{id}) + k_2 r_{2d}(gBest_d - x_{id})$$
$$V_{id} = \begin{cases} V_d^{max} \;, & v_{id} > V_d^{max} \\ -V_d^{max} \;, & v_{id} < -V_d^{max} \end{cases}$$
$$x_{id} = x_{id} + v_{id} \tag{11}$$

where w is inertia weight. k_1 and k_2 are two positive constants that represent the cognitive and social acceleration factors, respectively. r_{1d} and r_{2d} are random numbers uniformly distributed within the range [0,1]. $pBest_{id}$ denotes the position with the best fitness value, detected so far for the i^{th} particle. $gBest$ represents the best position obtained by the population. Furthermore, $V_{imax} = (v_{i1}^{max}, v_{i2}^{max}, \dots, v_{iD}^{max})$ represents an upper bound on the absolute amount of the velocity of the i^{th} particle.

Vol. 4(13), Oct, 2014, pp. 1452-1472, **ISSN**: 2305-0543
Available online at: http://www.aeuso.org

4.2. Fitness function

In order to find the optimal parameters of the controller PSO algorithm is employed. Indeed, the objective is to obtain the values of controller gains such that the objective function is minimized. In this paper, the mean of root of squared error is considered as the cost function, which for i^{th} sample is as follows:

$$MRSE = E(k) = \frac{1}{N}\sum_{i=1}^{N}\sqrt{e_{l1}^2(i) + e_{l2}^2(i) + e_{l3}^2(i)} \tag{12}$$

where $e_{l1}(i), e_{l2}(i), e_{l3}(i)$, are the trajectory tracking error of i^{th} sample for the first, second and third joint of the robot. Meanwhile, N is the number of samples and k is the iteration number.

5. Simulation Results

In this section, two different types of controllers including twisting algorithm and RISE feedback are designed for the tracking control of a three link robot manipulator. Numerical simulations are carried out using the Matlab software and the performances of these controllers are then compared. Consider the robot system introduced in section 2. The numerical values of the robot manipulator parameters are listed in Table 1

Table 1: Simulation parameters of robot

	Mass (m_i, Kg)	Link (a_i, m)	Moment of inertia (I_{oi}, Kgm^2)
Joint 1	1.2	0.5	43.33×10^{-3}
Joint 2	1.5	0.4	25.08×10^{-3}
Joint 3	3.0	0.3	32.67×10^{-3}

Vol. 4(13), Oct, 2014, pp. 1452-1472, **ISSN**: 2305-0543
Available online at: http://www.aeuso.org

The desired trajectory to be tracked by links is considered as $q_d = \left[\sin(t)\cos(t)\sin\left(t + \left({}^{\pi}/_{3}\right)\right)\right]^T$. Furthermore external disturbances of $\tau_{d1} = 0.2\sin(2t)$, $\tau_{d2} = 0.1\cos(2t)$, $\tau_{d3} = 0.1\sin(t)$ are applied to the system. Initial position and velocity of the joints are set to zero.

PSO algorithm is applied to tune the parameters of the twisting and RISE feedback controllers. According to [34], χ which is called the constriction factor, is defined as follows:

$$\chi = \frac{2}{\varphi - 2 + \sqrt{\varphi^2 - 4\varphi}} \ , \varphi = \varphi_1 + \varphi_2 \ , \varphi > 4 \tag{13}$$

In PSO algorithm, the parameters χ , φ_1, φ_2 are set to $0.7298, 2.05, 2.05$, respectively. The parameters w, k_1, k_2 are defined according to the following equations:

$$w = \chi \ , k_1 = \chi\varphi_1 \ , k_2 = \chi\varphi_2 \tag{14}$$

Numerical values of tuning parameters of the PSO algorithm are shown in Table 2.

Table 2: PSO tuning parameters

Parameter	Value
Population Size	20
No. of Iterations (k)	50
v_{max}	3
w	0.7298
k_1	1.4962
k_2	1.4962
Lower Bound	0
Upper Bound	35

International Journal of Mechatronics, Electrical and Computer Technology

Vol. 4(13), Oct, 2014, pp. 1452-1472, **ISSN**: 2305-0543
Available online at: http://www.aeuso.org

Case A. Twisting controller:

The twisting controller is designed according to the control torque input given in (10). The values of the twisting controller parameters obtained using PSO algorithm are given in Table 3.

Table 3: The gains of twisting controller

c_1	c_2	Best Cost
32	18.2	0.001629

Figures 3 to 6 depict the simulation results of the twisting controller. The convergence of objective functions is shown in figure 3.

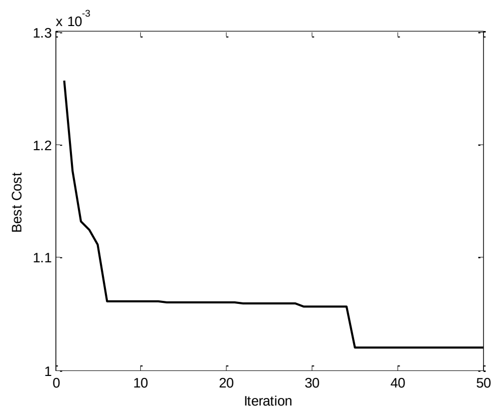

Figure 3. Fitness function values for 50 iterations

International Journal of Mechatronics, Electrical and Computer Technology

Vol. 4(13), Oct, 2014, pp. 1452-1472, **ISSN**: 2305-0543

Available online at: http://www.aeuso.org

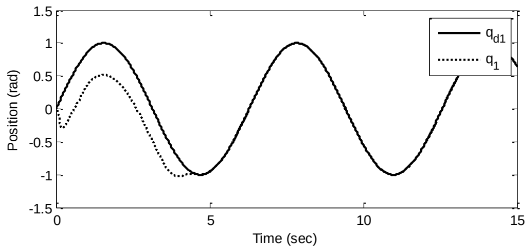

4(a). Trajectory tracking of joint angle 1

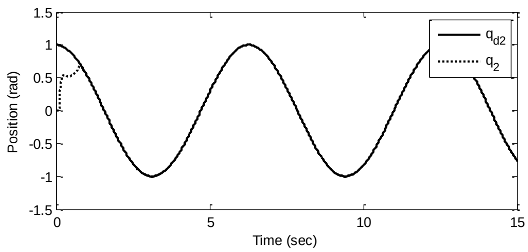

4(b). Trajectory tracking of joint angle 2

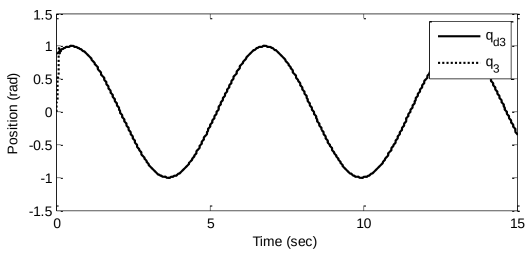

4(c). Trajectory tracking of joint angle 3

Figure 4. Tracking position of joints 1, 2 and 3

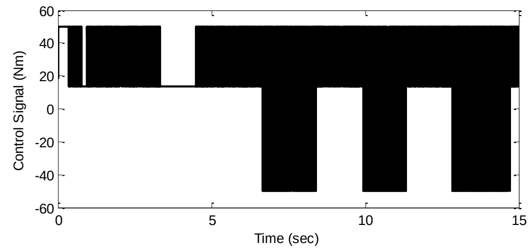

5(a). Control input for joint 1

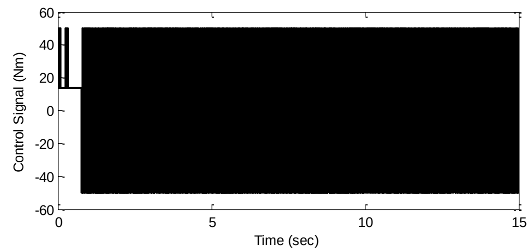

5(b). Control input for joint 2

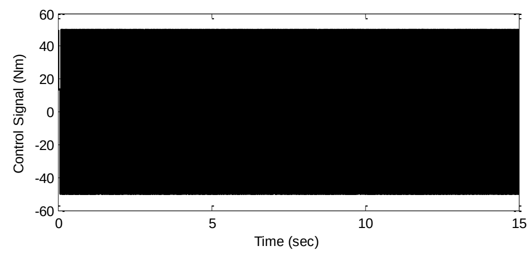

5(c). Control input for joint 3

Figure 5. Control input of joints 1, 2 and 3

International Journal of Mechatronics, Electrical and Computer Technology

Vol. 4(13), Oct, 2014, pp. 1452-1472, **ISSN**: 2305-0543

Available online at: http://www.aeuso.org

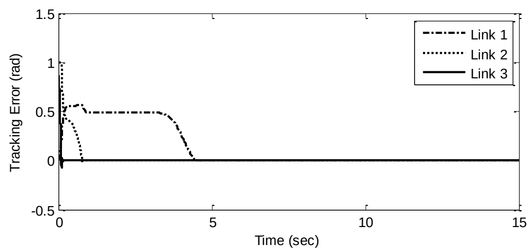

Figure 6. Tracking error of joints 1, 2 and 3

Figures 4(a) to 4(c) show the tracking performance of the twisting method. The twisting controller could suppress the uncertainties and external disturbances, so the system could track the desired trajectory. The control torque inputs applied to links 1, 2 and 3 are shown in figures 5(a) to 5(c). Figure 6 demonstrates the position tracking errors of links 1, 2 and 3. It can be seen that the second-order sliding mode twisting controller could afford the control objective in case of tracking error. However, the existence of discontinuous signum function in the control law results in chattering phenomenon, the destructive high-frequency oscillations in control signal.

Case B. RISE feedback controller

The RISE controller is applied on the robot system according to the control torque input presented in (8). Table 4 shows the RISE controller gains acquired using PSO algorithm.

Table 4. The gains of RISE feedback controller

k_s	β_1	α_2	Best Cost
25.32	16.7	29.3	0.001139

The simulation results of the RISE controller are shown in figures 7 to 10.

Vol. 4(13), Oct, 2014, pp. 1452-1472, **ISSN**: 2305-0543
Available online at: http://www.aeuso.org

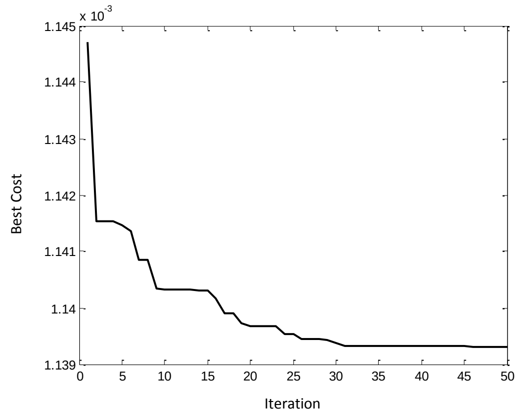

Figure 7. Fitness function values for 50 iterations

Figure 7 shows the fitness function trend, which is reduced to find the gain values of the RISE controller.

International Journal of Mechatronics, Electrical and Computer Technology

Vol. 4(13), Oct, 2014, pp. 1452-1472, **ISSN**: 2305-0543

Available online at: http://www.aeuso.org

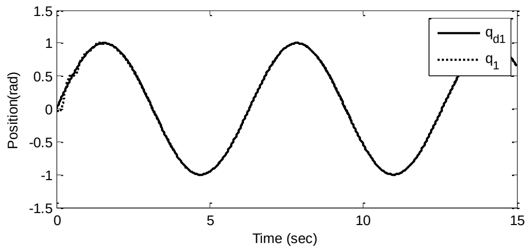

8 (a). Trajectory tracking of joint angle 1

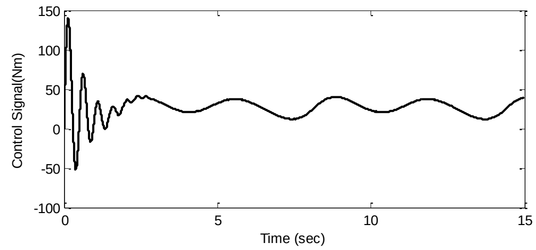

9 (a). Control input for joint 1

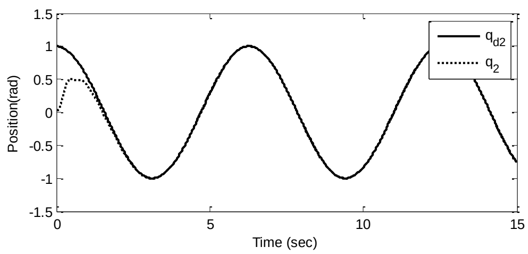

8 (b). Trajectory tracking of joint angle 2

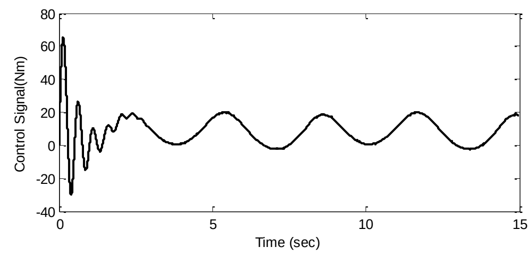

9 (b). Control input for joint 2

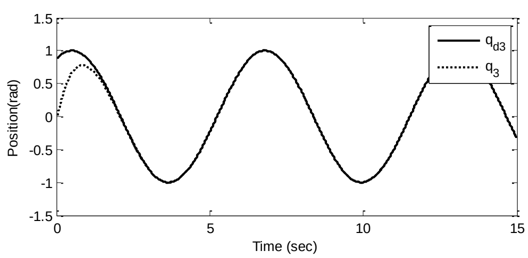

8 (c). Trajectory tracking of joint angle 3

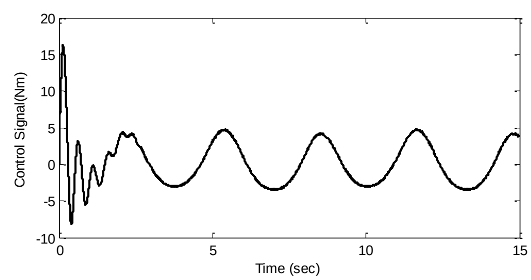

9 (c). Control input for joint 3

Figure 8. Tracking position of joints 1, 2 and 3

Figure 9. Control input of joints 1, 2 and 3

Vol. 4(13), Oct, 2014, pp. 1452-1472, **ISSN**: 2305-0543
Available online at: http://www.aeuso.org

The trajectory tracking simulation results of all three joints of the robot and their corresponding control inputs applied to the system are shown in figures 8 and 9. As it can be seen from the figures, the control objective is successfully achieved. Furthermore, the proposed controller generates a continuous control signal, which prevents chattering phenomenon. In fact, the existence of a unique integral sign term in the RISE controller causes a continuous control structure which avoids the occurrence of chattering phenomenon that usually happens in sliding mode controllers.

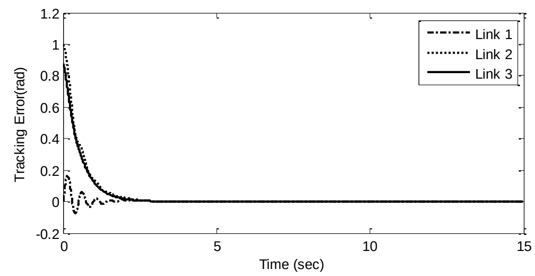

Figure 10. Tracking error of joints 1, 2 and 3

Figure 10 indicates the position tracking error for all three links of the robot, which confirms that asymptotic tracking is achieved even with the external disturbances.

Conclusion

In this paper, two different controllers including RISE feedback and twisting second-order sliding mode are successfully designed for trajectory tracking control of a three link robot manipulator in presence of uncertainties and external disturbances. An intelligent tuning of the controllers parameters is conducted by using particle swarm optimization algorithm. The parameters of the controllers are adjusted while PSO minimizes the mean of root of squared error. Based on the simulation results, a conclusion has been made that both of the control methods are highly robust against uncertainties and external disturbances. The simulation

Vol. 4(13), Oct, 2014, pp. 1452-1472, **ISSN**: 2305-0543
Available online at: http://www.aeuso.org

results have shown also that the RISE feedback controller can compensate for uncertainties without any chattering in the control input in comparison with the twisting controller. Indeed, the existence of a unique integral sign term in this method prevents the occurrence of undesirable chattering phenomenon. Moreover, this control scheme can be applied to nonlinear systems with arbitrary relative degree, unlike twisting algorithm which is limited to plants with relative degree two.

References

[1] Le T. D., Kang H.-J., Suh Y.-S. and Ro Y.-S (2012) An Online Self Gain Tuning Method Using Neural Networks for Nonlinear PD Computed Torque Controller of a 2-dof Parallel Manipulator, Neurocomputing.

[2] Xiaocong Z., Guoliang T., Bin Y. and Jian C. (2009) Integrated Direct/Indirect Adaptive Robust Posture Trajectory Tracking Control of a Parallel Manipulator Driven by Pneumatic Muscles. Control Systems Technology, IEEE Transactions on, vol. 17, pp. 576-588.

[3] Kamnik R, Matko D, Bajd T (1998) Application of model reference adaptive control to industrial robot impedance control. Journal of Intelligent & Robotic Systems; 22(2):153-163.

[4] Sadati N. and Ghadami R. (2008) Adaptive multimodel sliding mode control of robotic manipulators using soft computing. Neurocomputing, vol. 71, pp. 2702-2710.

[5] Zeinali M. and Notash L. (2010) Adaptive sliding mode control with uncertainty estimator for robot manipulators. Mechanism and Machine Theory, vol. 45, pp. 80-90.

[6] X. Chen, T. Fukuda: Robust sliding-mode tip position control for flexible arms, IEEE Trans. Ind. Electron, 48(6), 1048–1056, (2001).

[7] Ciliz M. K. (2005) Adaptive control of robot manipulators with neural network based compensation of frictional uncertainties. Robotica, vol. 23, pp. 159-167.

[8] Wang L, Chai T, Yang C (2012) Neural-Network-Based Contouring Control for Robotic Manipulators in Operational Space.

[9] S.J. Huang, J.S. Lee, A stable self-organizing fuzzy controller for robotic motion control, IEEE Trans. Ind. Electron. 47 (2000) 421.

[10] Edwards C, Spurgeon SK. *Sliding Mode Control: Theory and Applications*. Taylor and Francis, 1998.

[11] Utkin VI, Guldner J, Shi J. *Sliding Mode Control in Electro-Mechanical Systems*, Second Edition. CRC Press, 2009.

Vol. 4(13), Oct, 2014, pp. 1452-1472, **ISSN**: 2305-0543

Available online at: http://www.aeuso.org

[12] A. I. Bhatti, S. K. Spurgeon, R. Dorey, and C. Edward. Sliding mode configuration for automotive control. *Int. J. Adapt. Control Signal Process*, 13:49–69, (1999).

[13] S. V. Emelyanov, "Variable structure control systems (in Russian)," Moscow: Nauka, 1967.

[14] Emel'yanov, S.V., S.K. Korovin, and A. Levant, "High-Order Sliding Modes in Control Systems," *Comput. Math. Mode.*, Vol. 7, No. 3, pp. 294-318 (1996).

[15] G. Bartolini, A. Levant, A. Ferrara, E. Usai, "Higher Order Sliding Modes for the Output-Feedback Control of Nonlinear Uncertain Systems In Variable Structure Systems:" In X.Yu and J.-X.Xu (Eds.) *Towards the 21st Century (Lecture Notes in Control and Information Sciencz, 274*), London, Springer Verlag, pp. 83-108, 2002.

[16] Sira-Ramirez, H. (2002). Dynamic second-order sliding mode control of the hovecraft vessel. *IEEE Transactions on Control System Technology*, *10*(6), 860–865.

[17] Damiano A, Gatto GL, Marongiu I, et al. Second-order sliding-mode control of DC drives. IEEE Trans Ind Electron 2004; 51: 364–373.

[18] Mihoub M, Nouri AS, Abdennour RR. Real-time application of discrete second order sliding mode control to a chemical reactor. Control Eng Pract 2009;17: 1089_95.

[19] Van M, Kang HJ and Suh YS. Output feedback tracking control of uncertain robot manipulators via highorder sliding mode observer and fuzzy compensator. J Mech Sci Technol 2013; 27(8): 2487–2496.

[20] Bartolini, G., Pisano, A., Punta, E., & Usai, E. (2003). A survey of appplications of second order sliding mode control to mechanical systems. *International Journal of Control*, *76*(9/10), 875–892.

[21] G. Bartolini, A. Ferrara, A. Levant, E. Usai, "On Second Order Sliding Mode Controllers", In K.D. Young and U. Ozguner (eds.) *Variable Structure Systems, Sliding Mode and Nonlinear (Lecture Notes in Control and Information Science, 247)*, London: Springer-Verlag, pp. 329-350, 1999.

[22] Bartolini G, Farrara A, Usai E. Applications of sub-optimal discontinuous control algorithm for uncertain second order systems. Internat J Robust Nonlinear Control 1997;7:299_319.

[23] Perruquetti W, Barbot JP. Sliding mode control in engineering. In: Automation and control series. New York (USA): Marcel Dekker Inc.; 2002.

[24] B. Xian, D.M. Dawson, M.S. de Queiroz and J. Chen, "A continuous asymptotic tracking control strategy for uncertain multi-input nonlinear systems," *IEEE Transactions on Automatic Control*, 49 (2004) 1206–1211.

[25] C. Makkar, G. Hu, W. G. Sawyer, and W. E. Dixon, "Lyapunov-based tracking control in the presence of uncertain nonlinear parameterizable friction," *IEEE Trans. Automat. Control*, 52 (2007).

[26] Z. Cai, M. S. de Queiroz, and D. M. Dawson, "Robust adaptive asymptotic tracking of nonlinear systems with additive disturbance," *IEEE Trans. Automat. Control*, 51(3) (2006).

International Journal of Mechatronics, Electrical and Computer Technology

Vol. 4(13), Oct, 2014, pp. 1452-1472, **ISSN**: 2305-0543

Available online at: http://www.aeuso.org

[27] P.M. Patre, W. MacKunis, W.E. Dixon, "Asymptotic tracking for uncertain dynamic systems via a multilayer NN feedforward and RISE feedback control structure," *IEEE Transactions on Automatic Control*, 53(9) (2008) 2180–2185.

[28] W. MacKunis, P. M. Patre, M. K. Kaiser, and W. E. Dixon, "Asymptotic tracking for aircraft via robust and adaptive dynamic inversion methods," *IEEE Trans. Cont. Syst. Technol*, 18(6) (2010).

[29] P. M. Patre, W. MacKunis, C. Makkar, and W. E. Dixon, "Asymptotic tracking for systems with structured and unstructured uncertainties," *IEEE Trans. Cont. Syst. Technol*. 16(2) (2008).

[30] S. Wang, H. Min, F. Sun, J. Zhang, "Neural Network Control of Spacecraft Formation Using RISE Feedback," *Advances in Neural Network Research and Applications*, vol. 67, pp. 521– 528, 2010.

[31] M. Spong, M. Vidyasagar, Robot Dynamics and Control, John Wiley and Sons, Inc., 1989.

[32] E. Kim: Output feedback tracking control of robot manipulators with model uncertainty via adaptive fuzzy logic, IEEE Trans. Fuzzy Systems, **12**(3), 368–378, (2004).

[33] Igor Boiko, Ivan Castellanos, and Leonid Fridman, " Analysis of response of second-order sliding mode controllers to external inputs in frequency domain", Int, J. Robust nonlinear control, Vol.18, pp 502-514, 2008.

[34] M. Clerc and J. Kennedy, "The Particle Swarm—Explosion, Stability, and Convergence in a Multidimensional Complex Space", *IEEE Transactions on Eevolutionary Computation*, vol. 6, no. 1, February, 2002.